Preprints (www.preprints.org) | NOT PEER-REVIEWED | Posted: 14 June 2019 doi:10.20944/preprints201906.0136.v1

Technical Note

On the precise examination of multi-port antennas; corrections and criticisms to some recently reported results

Mahdi Fartookzadeh [1,*]

[1] Electrical and Computer Engineering Complex, Malek Ashtar University, Tehran, Iran; Mahdi.fartookzadeh@gmail.com

* Correspondence: Mahdi.fartookzadeh@gmail.com

Abstract: In this paper, precise examination of multi-port antennas with large mutual coupling between the ports is studied. For this purpose, some vital parameters such as active reflection coefficients and realised gain are emphasized. The main motivation of this research is the ignorance of this issue in several recently published papers. Hence, corrections and criticisms to some recently reported results are presented. At first, a microstrip patch consisting of two inverted U-slots is re-examined, which has been proposed in a recently published paper for wideband applications. However, the authors did not present satisfactory results to indicate the performance of the proposed structure. In reverse, some important parameters such as the antenna gain appear to be incorrectly reported. In this paper, the characteristics of the antenna are compared with a simple 50 Ω microstrip line excited by two probes, indicating no significant differences. In the remainder of this paper, some corrections are provided on two examples of wide-beam circularly polarised multi-fed antennas for satellite applications. The first example is the multi-fed spiral antennas with folded arms, which have been proposed as the widebeam antennas at 435 MHz. It is indicated that the antenna height should be increased for better performance. The second example is the quadrifilar square helical antennas with folded arms, which have been proposed as the widebeam antennas for 435 MHz with minor responses at 145 MHz. Some corrections are presented on the previously reported minor responses at 145 MHz.

Keywords: Active reflection coefficients; realised gain; multi-port antennas; U-slotted microstrip patch; quadrifilar helical antennas.

1. Introduction

Mutual-coupling is a well-studied topic in the design and investigation of linear, planar and conformal antenna arrays, having vital effects on the performance. A consequence of mutual coupling effects is the appearance and transfer of maximums and nulls in the radiation pattern [1-3]. Although, the effects are usually undesirable for arrays and other applications, they are not always destructive for multi-port antennas, such as wide-beam circularly polarised antennas [4].

Nevertheless, it is important to remember that the evaluation of multi-port antennas is different from one-port antennas. For example, the bandwidth of -10 dB reflection coefficient is usually considered as the bandwidth of one-port antennas. In addition, the value of the antenna gain is similar with the realised gain at this frequency band. However, as well as the reflection coefficient, isolation between the inputs should be examined for multi-port antennas, to indicate the structure is radiating, instead of transmitting the power from one port to another one. To prevent from ignorance of the coupling effects between antenna ports, the active reflection coefficients (active S-parameters) and the realised gain should be examined as well as the reflection coefficients and the gain [5]. This is in fact not a new finding and it has been reflected in several papers such as [6-8]. However, the ignorance of this issue in several other papers [9-22] is the motivation of this research to prevent from further errors.

© 2019 by the author(s). Distributed under a Creative Commons CC BY license.

Preprints (www.preprints.org) | NOT PEER-REVIEWED | Posted: 14 June 2019 doi:10.20944/preprints201906.0136.v1

Above all, while looking for a wideband microstrip antenna in the recently published papers, I encountered to a significant solution, an octave-bandwidth antenna consisting of two inverted U-slots and two probes [9]. This could be a ground-breaking improvement in this field, as can be observed in table II of [9]. Specifically, the proposed antenna in [9] is demanded to have significant performance improvement with significant reduction of substrate thickness, compared with the prior works. However, re-examination of the proposed structure in [9] indicated that it is not a good radiating element at all. For this purpose, the performance of the antenna is compared with a simple 50 Ω microstrip line excited by two probes in section 2, indicating no significant differences.

Examination of miniaturised wide-beam antennas with circular polarisation (CP) for satellite applications is the next topic in this paper. These antennas usually have multiple ports with the same angular and phase differences between them. Therefore, considering the active S-parameters and the realised gain is necessary for these antennas. In fact, the original antennas such as quadrifilar helical antennas (QHAs) and conical QHAs have proven in the past to be reliable. However, the issue is more important when the antennas are miniaturised, since the coupling between the ports is increased, such as for the QHAs with meandered or folded arms, the conical QHAs with folded arms, etc. [12-20]. In this paper, two structures are re-examined; multi-fed spiral antennas with folded arms [21, 22] in section 3 and quadrifilar square helical antennas (QSHAs) with folded arms [4] in section 4. It is indicated that the situation is better for these antennas compared with the U-slotted microstrip patch, since the differences between the gain and the realised gain are very less at the operating frequencies. However, the realised gains of the QSHAs at 145 MHz are reduced significantly due to the fundamental limitations for the gain of an antenna.

2. Microstrip patch with two inverted U-slots vs. microstrip transmission line

Schematic of the proposed structure in [9] is indicated in Fig. 1(a). It contains two coaxial probes on a single patch and two inverted U-slots. The authors of [9] determined the antenna bandwidth from the reflection coefficient. However, as well as the reflection coefficient, isolation between the two inputs should have been examined, to indicate that the structure is radiating, instead of transmitting the power from one input to the other one. The effects of this ignorance can be observed on the realised gain and active$S$-parameters as will be indicated, subsequently. Furthermore, the performance of the antenna is compared with a simple 50 Ω microstrip line excited by two probes, as depicted in Fig. 1(b). Separation between the probes, thickness of the substrate, h, and relative permittivity, ϵ_r, are similar to the U-slotted patch ($h = 1.57$ mm and $\epsilon_r = 2.2$). ANSYS HFSS is used for all simulations in this paper [23].

At first, the current distributions on the 50 Ω microstrip line and the radiation patterns are studied when the two probes are excited in-phase (difference mode) and with 180° out-of-phase (sum mode). The current distributions are depicted in Fig. 2 at 3.5 GHz for both situations, indicating similar behaviour as Fig. 13 of [9]. In addition, the radiation patterns of the U-slotted microstrip patch are compared with the 50 Ω microstrip line in Fig. 3(a) and Fig. 3(b) at sum and difference modes, respectively. It can be observed that the radiation characteristics of the two structures are very similar at 3.5 GHz. The performance is almost similar throughout the bandwidth, 2 GHz to 4 GHz. The frequency responses of the two structures are compared in the following figures.

Reflection coefficients, S_{11}, and transmission coefficients, S_{12}, of the two structures are compared in Fig. 4. An octave bandwidth can be observed for the reflection coefficients of the U-slotted patch, similar to the results indicated in Fig. 17 of [9]. However, the reflection coefficient bandwidth of the microstrip transmission line is considerably wider. Hence, this is not enough for judging the performance of a two-input structure as an antenna. For this purpose, the transmission coefficients should be studied as well. It can be observed in Fig. 4 that the transmission coefficients of both structures are near zero (dB), leading to low radiation efficiencies. This also results in large differences between gain and realised gain, since the effects of scattering parameters are applied on

Preprints (www.preprints.org) | NOT PEER-REVIEWED | Posted: 14 June 2019 doi:10.20944/preprints201906.0136.v1

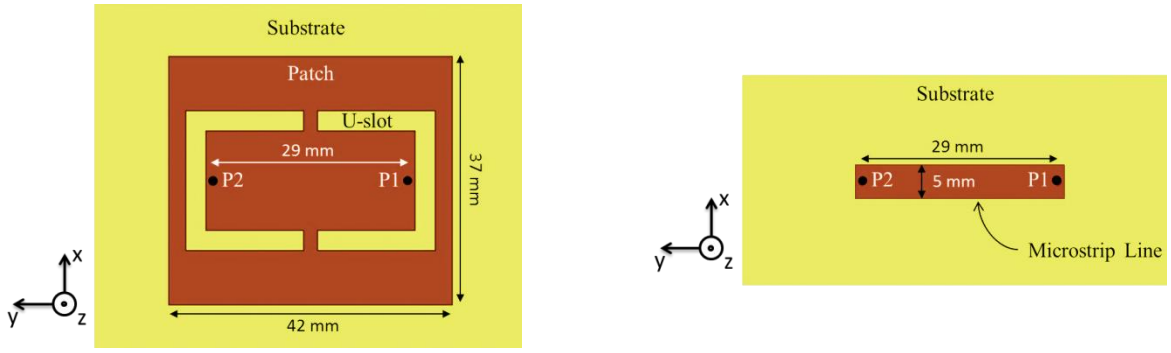

(a) (b)

Figure 1. Schematics of the structures with two probes for constructing monopulse-like radiation patterns; (a) the proposed patch antenna consisting two inverted U-slots in [9], and (b) a 50 Ω microstrip line on a same substrate with two probes having a similar separation.

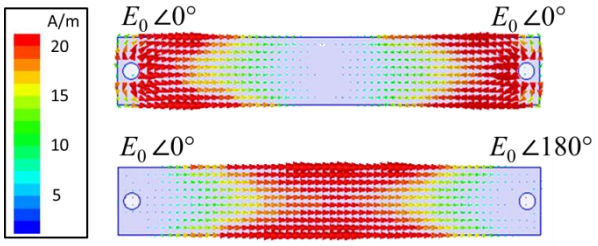

Figure 2. Current distributions on the 50 Ω microstrip line when the two probes are excited in-phase (difference mode) and out-of-phase (sum mode).

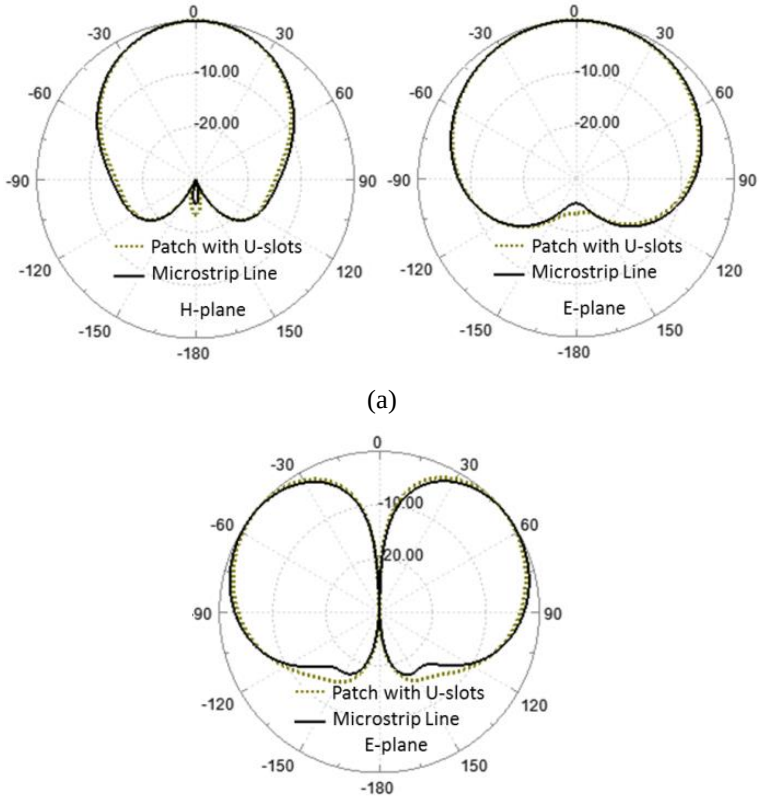

(a)

(b)

Figure 3. Radiation patterns of the U-slotted microstrip patch compared with the 50 Ω microstrip line when the two probes are excited (a) out-of-phase at h-plane, $\phi = 0°$, and e-plane, $\phi = 90°$, (sum mode), and (a) in-phase at e-plane, $\phi = 90°$ (difference mode).

Preprints (www.preprints.org) | NOT PEER-REVIEWED | Posted: 14 June 2019 doi:10.20944/preprints201906.0136.v1

the realised gain in simulations instead of the gain. However, it could be recognized if the measured gain of the fabricated prototype has been reported in [9].

Nevertheless, simulated maximum gains and realised gains of the structures are indicated in Fig. 5(a) and (b) at sum and difference modes, respectively. In both situations and for both structures substantial differences can be observed between the gain and the realised gain. Furthermore, the gain and the realised gain of the U-slotted microstrip patch are significantly reduced on most of the bandwidth in comparison with a simple 50 Ω transmission line, at difference mode.

Another viable factor for analysing the performance of multi-input antennas is the active S-parameter which recounts the effects of the scattered waves from other ports as well as the reflected wave [5]. The definition for the i-th port of an antenna with N ports is

$$Active\ S_i = \sum_{j=1}^{N} \frac{a_i}{a_j} S_{ij}, \tag{1}$$

where a_j is the amplitude of the j-th element, $i, j = 1,2, \dots, N$. For the symmetric structures indicated in Fig. 1, active S_1 and active S_2 are similar. Therefore, active S_1 is only illustrated in Fig. 6 for both structures at sum and difference modes. It can be observed that the power is returning to the input ports and no significant radiation is occurring at both situations. Only a narrowband resonance is observed for the U-slotted microstrip patch at the difference mode on 4 GHz, wherein the realised gain meets the gain (see Fig. 5(b)).

Consequently, the proposed structure in [9] is more similar to a transmission line on the frequency band, 2-4 GHz, instead of a broadband antenna. The rest of this paper is about the two recently proposed structures as the miniaturised circularly polarised wide-beam antennas for satellite application.

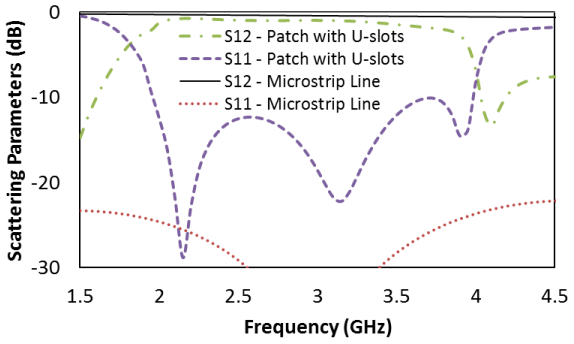

Figure 4. Scattering parameters of the microstrip patch with two inverted U-slots compared with the microstrip line.

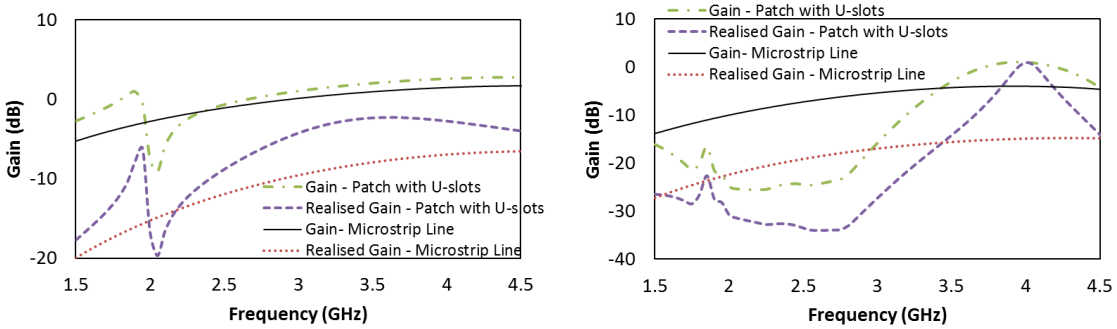

(a) (b)

Figure 5. Comparison between maximum gains and realised gains of the microstrip patch with two inverted U-slots and the microstrip line at two situations; (a) sum mode and (b) difference mode.

Preprints (www.preprints.org) | NOT PEER-REVIEWED | Posted: 14 June 2019 doi:10.20944/preprints201906.0136.v1

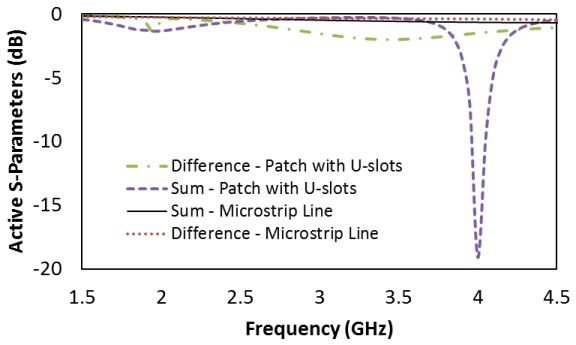

Figure 6. Comparison between active S-parameters of the microstrip patch with two inverted U-slots and the microstrip line.

3. Multi-fed spiral antennas with folded arms

Miniaturised spiral antennas with three folded arms have been proposed in [21] for satellite applications. It is also indicated that the antenna can be design with four or six number of arms in [22]. Furthermore, the effects of changing the heights of these antennas on the radiation patterns are studied in [22]. However, the analyses in [21, 22] are not complete, since the active S-parameters and the realised gain are not reported. In this section these parameters are studied and the method of improvement is explained.

Schematics, top view and side view, of the left-hand circularly polarised (LHCP) triple-fed spiral antenna on a substrate with $\epsilon_r = 2.55$ are depicted in Fig. 7. The structure can be mirrored to construct a right-hand circularly polarised (RHCP) antenna. S_{11} and active S_1 of the antenna with the dimensions $[R_2 = 116.5,\ R_p = 101,\ R_1 = 19,\ h = 50]$ mm are indicated in Fig. 8(a). Scattering parameters of the other ports are similar, due to the symmetric structure. The amplitudes and phases of all inputs are indicted in Fig. 7 ($E_0 = 1$). It can be observed that the S_{11} is below -10 dB from 430 MHz to 450 MHz, indicating low-level reflection coefficient. However, active S_1 is larger than -6 dB, leading to a significant difference between the gain and the realised gain of the antenna. In particular, the difference between the gain and the realised gain is 2 dB at 435 MHz and 1.3 dB at 430 MHz, as can be observed in Fig. 8(b). The difference indicates that some part of the excited power is transmitted from one port to another, instead of being radiated.

In order to improve the radiation efficiency and reduce the active S-parameters, the simplest method is to increase the height of antenna. For example, if the antenna height is increased to 100 mm, and the other dimensions are adjusted at $[R_2 = 108.6,\ R_p = 94,\ R_1 = 17.8]$ mm to keep the resonance frequency on 435 MHz, the S_{11} and active S_1 will be as depicted in Fig. 9(a). It can be observed that the active S_1 is below -10 dB at 435 MHz as well as the S_{11}. In addition, the gain and the realised gain are depicted in Fig. 9(b), indicating a good agreement at 435 MHz.

As a final point in this section, the radiation patterns are depicted in Fig. 10. Comparison between the gains at 435 MHz in Fig. 10(a) indicates a small improvement of the beamwidth when the antenna height is increased [22]. However, the difference is more apparent between the realised gains in Fig. 10(b), since the increase of the antenna height improved the performance, significantly.

Preprints (www.preprints.org) | NOT PEER-REVIEWED | Posted: 14 June 2019 doi:10.20944/preprints201906.0136.v1

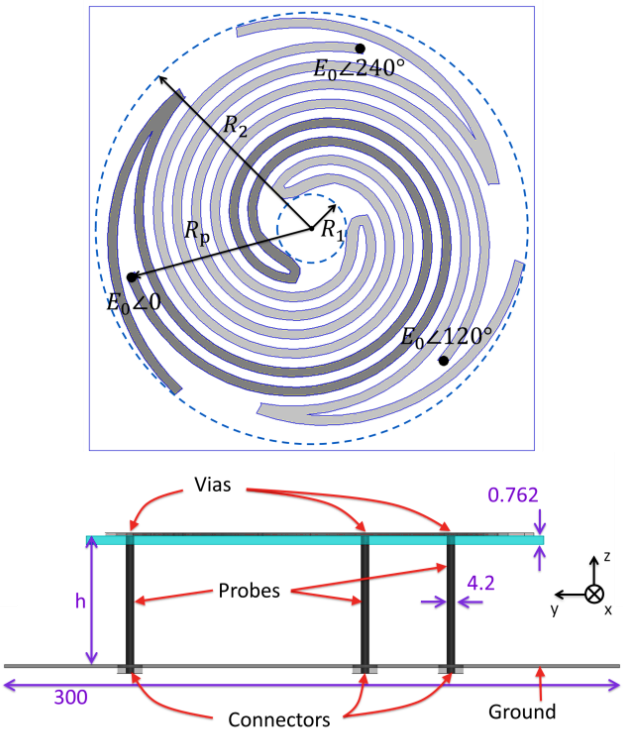

Figure 7. Schematics, top view and side view of the triple-fed spiral antenna with folded arms [21]

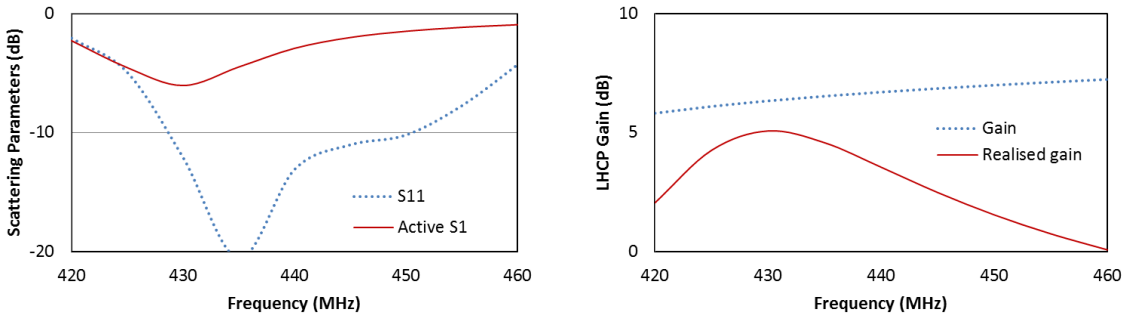

(a) (b)

Figure 8. Simulation results of the triple-fed spiral antenna with h = 50 mm; (a) S_{11} compared with active S_1, and (b) the gain compared with the realised gain.

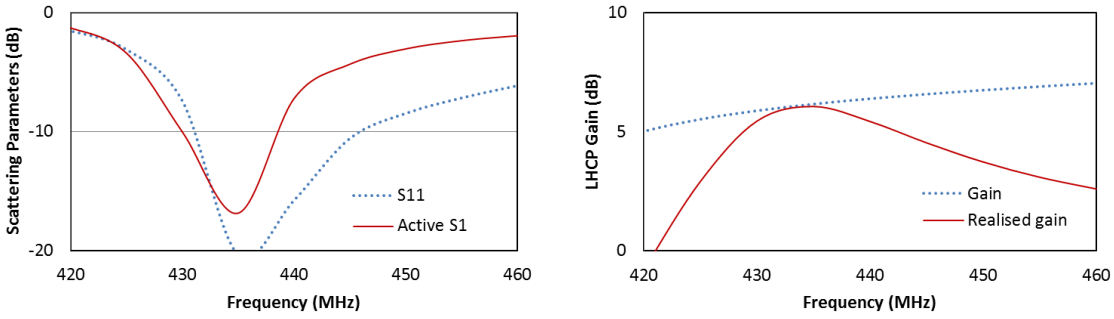

(a) (b)

Figure 9. Simulation results of the triple-fed spiral antenna with h = 100 mm; (a) S_{11} compared with active S_1, and (b) the gain compared with the realised gain.

Preprints (www.preprints.org) | NOT PEER-REVIEWED | Posted: 14 June 2019 doi:10.20944/preprints201906.0136.v1

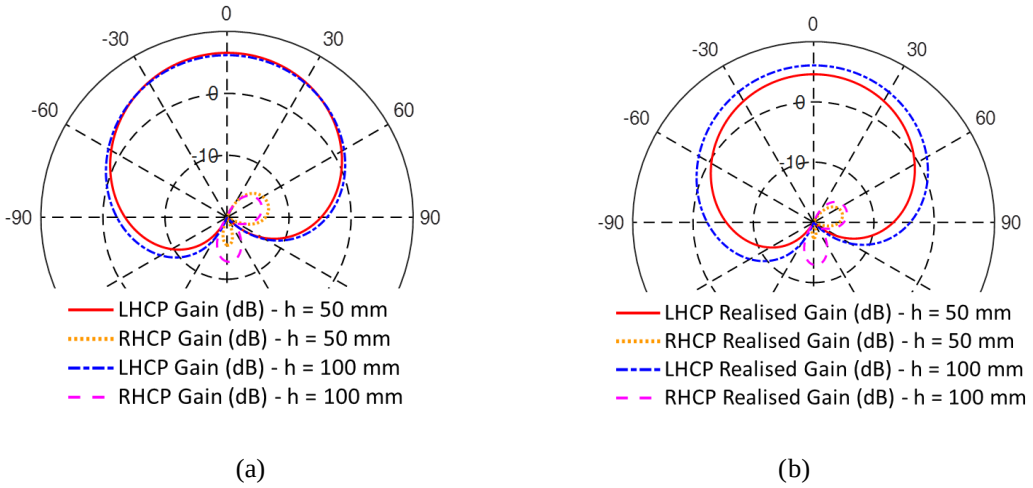

(a) (b)

Figure 10. Simulated radiation patterns of the triple-fed spiral antennas at f = 435 MHz with h = 50 mm and h = 100 mm; (a) the gain and (b) the realised gain.

4. Miniaturised QSHAs

Two versions of the QSHAs have been proposed for satellite applications in [4], with the operating frequency of 435 MHz and minor responses at 145 MHz. Arms of the first antenna are isolated, while the second antenna has connected arms as indicated in Fig. 7. Amplitudes of the input signals are the same with 90° out of phase with respect to each other similar to the traditional QHAs. The performances of both antennas at 435 MHz are verified by the measured results in [4]. However, the minor responses at 145 MHz are the concerns that should be more investigated.

At first, the scattering parameters of the small antenna are illustrated in Fig. 12(a), indicating that the active S_1 is about -0.7 dB at 145 MHz. It means that only 14.9 % of the excited signal is radiated and the rest is reflected to the inputs. Therefore, the realised gain should be 14.9 % of the gain which is in agreement with the gain plots in Fig. 12(b), wherein the realised gain is 8.3 dB less than the gain at 145 MHz. This is indeed in agreement with the well-known fundamental limitation of the gain of an antenna with the given dimensions. In particular, the maximum gain of an antenna with the area, A (in square meters), is given by $g_{max} = (4\pi/\lambda^2)A$, where λ is the wavelength in meters. Therefore, if we assume the antenna area as $A = 0.143^2$ (see Fig. 11(a)), we have $g_{max} = 0.06$ and $G_{max} = -12.2$ dB, which is very smaller than the value of gain at 145 MHz in Fig. 12(b). However, if the box area is assumed, $A = 0.25^2$, the maximum gain is $g_{max} = 0.36$ and $G_{max} = -4.44$ dB, which is again smaller than the value of gain at 145 MHz. Nevertheless, the maximum gain for the second assumption is larger from the simulated realised gain at 145 MHz in Fig. 12(b), indicating the possibility of obtaining this value of gain in the real situation.

Finally, simulation results of the large antenna in Fig. 11(b) are indicated in Fig. 13. Active S_1 is compared with S_{11} in Fig. 13(a), indicating that the active S_1 is about -2.9 dB at 145 MHz. Hence, the realised gain should be 48.7 % of the gain, since the rest is reflected to the input ports. This is also in agreement with the gain plots in Fig. 13(b), in which the realised gain is 3.1 dB less than the gain at 145 MHz. The maximum possible gains for this antenna are -7.36 dB and -2.26 dB assuming the antenna area, $A = 0.25^2$, and the holding box area, $A = 0.45^2$, respectively. It can be observed in Fig. 13(b) that the only feasible gain is the realised gain with the second assumption of the area.

Preprints (www.preprints.org) | NOT PEER-REVIEWED | Posted: 14 June 2019 doi:10.20944/preprints201906.0136.v1

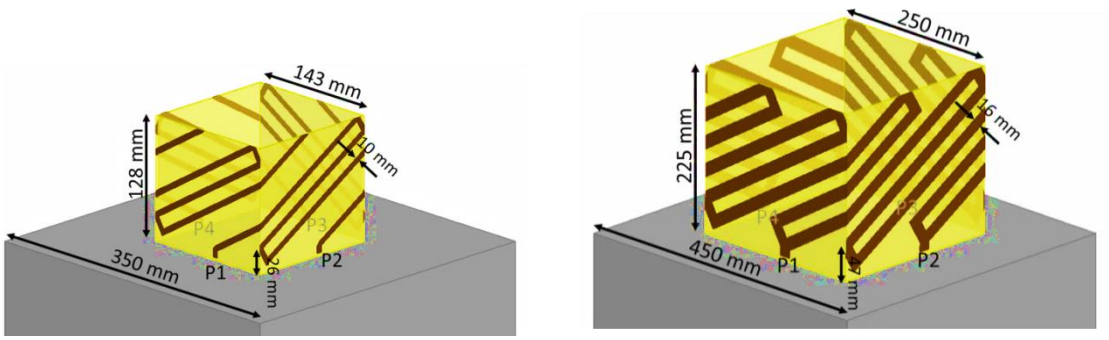

(a) (b)

Figure 11. Schematics of the proposed QSHAs in [4]; (a) the small antenna with isolated arms and 350 mm sides of the holding box and (b) the large antenna with connected arms and 450 mm sides of holding box.

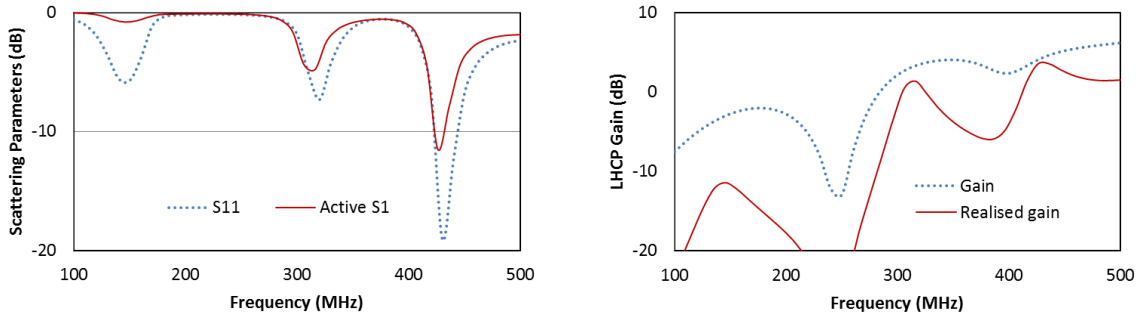

(a) (b)

Figure 12. Simulation results of the small QSHA; (a) S_{11} compared with active S_1, and (b) the gain compared with the realised gain.

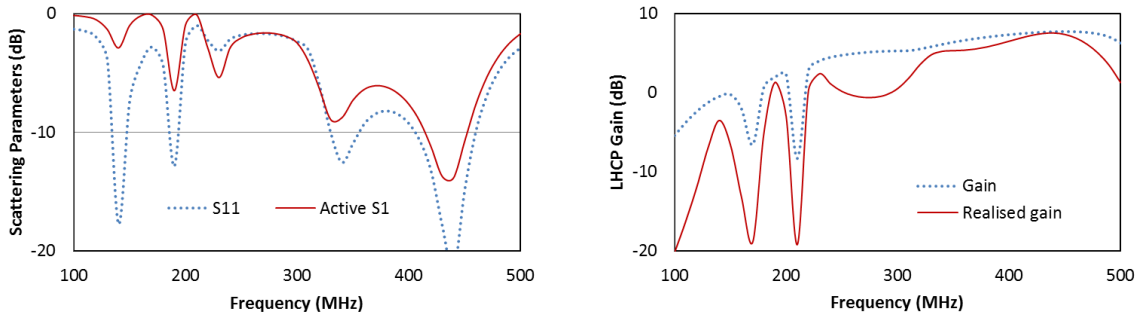

(a) (b)

Figure 13. Simulation results of the large QSHA; (a) S_{11} compared with active S_1, and (b) the gain compared with the realised gain.

5. Conclusions

The importance of considering active reflection coefficients and the realised gain as well as the reflection coefficients and the gain has been re-emphasized in this paper. The ignorance of these parameters in some recently published papers has been highlighted. In the beginning, a microstrip patch antenna consisting of two inverted U-slots has been studied, which has been proposed for wideband application recently. However, the performance of the antenna has been compared with a simple 50 Ω microstrip line excited by two probes, indicating no significant differences.

Preprints (www.preprints.org) | NOT PEER-REVIEWED | Posted: 14 June 2019 doi:10.20944/preprints201906.0136.v1

Subsequently, some corrections have been proposed on two examples of miniaturised wide-beam circularly polarised multi-fed antennas. As the first example, the multi-fed spiral antenna with folded arms has been studied, indicating that the antenna height should be increased for better performance. As the second example, the quadrifilar square helical antennas have been considered, which have been proposed as the widebeam antennas at 435 MHz with minor responses at 145 MHz. It is indicated that the previously reported gains of these antennas at 145 MHz are higher than the maximum possible gain due to the limited dimensions. In fact, the effects of active reflection coefficients were ignored in calculating the gains.

References

1. S. P. Skobelev, Phased Array Antennas with Optimized Element Patterns. Norwood, MA, USA: Artech House, 2011
2. R. J. Mailloux, Phased Array Antenna Handbook Norwood, MA, USA: Artech House, 2005
3. Balanis C. A., "Antenna Theory: Analysis and Design". Hoboken, NJ, USA: Wiley, 2005
4. Fartookzadeh, M. and Mohseni Armaki, S.H., "Printed quadrifilar square-helical antennas with folded arms for satellite applications", *IET Microwaves, Antennas & Propagation*, 2018, *12*(11), pp.1780-1785.
5. Craeye, C. and González-Ovejero, D., "A review on array mutual coupling analysis." *Radio Science*, 2011, *46*, (02), pp.1-25.
6. Liao, S., Xue, Q.: "Compact UHF three-element sequential rotation array antenna for satcom applications", *IEEE Trans. Antennas Propag.*, 2017, **65**, (5), pp. 2328–2338
7. Sun, L., Li, Y., Zhang, Z. and Feng, Z., "Low-Profile Compact Circularly-Polarized Slot-Etched PIFA Using Even and Odd Modes." IEEE Transactions on Antennas and Propagation. 2019
8. Inserra, D., Wen, G. and Hu, W., "Sequentially Rotated Circular Antenna Array With Curved PIFA and Series Feed Network". IEEE Transactions on Antennas and Propagation, 2018, 66, (11), pp.5849-5858.
9. Radavaram, S. and Pour, M.,: "Wideband Radiation Reconfigurable Microstrip Patch Antenna Loaded With Two Inverted U-Slots". *IEEE Transactions on Antennas and Propagation*, 2019, 67, (3), pp.1501-1508.
10. Soghi, S., Mohseni Armaki, S.H. and Fartookzadeh, M., 2017. Miniaturized dual-band PCB inverted F/L antenna for nano-satellite application. *Microwave and Optical Technology Letters*, *59*, (11), pp.2898-2903.
11. Tae, H.S., Oh, K.S., Son, W.I., *et al.*: "Design of compact dual-band quadruple inverted-F/L antenna for GPS L1/L2 band", *IEEE Trans. Antennas Propag.*,2013, **61**, (4), pp. 2276–2279
12. Fartookzadeh, M., Armaki, S.M.: "Multi-band conical and inverted conical printed quadrifilar helical antennas with compact feed networks", *AEU-Int. J. Electron. Commun.*, 2016, **70**, (1), pp. 33–39
13. Khajepour, S., Ghaffarian, M.S., Moradi, G.: "Design of novel multiband folded printed quadrifilar helical antenna for GPS/WLAN applications", *Electron. Lett.*, 2016, **53**, (2), pp. 58–60
14. Chiu, C.W., Ou, C.A. and Wang, H.C., "Compact printed quadrifilar helix antenna for universal RFID hand-held reader", *Journal of Electromagnetic Waves and Applications*, 2015, *29*, (7), pp.891-904.
15. Tawk, Y., Chahoud, M., Fadous, M., Costantine, J. and Christodoulou, C.G. "The miniaturization of a partially 3-D printed quadrifilar helix antenna". *IEEE Transactions on Antennas and Propagation*, 2017, *65*(10), pp.5043-5051.
16. Qu, M., Deng, L., Li, M., Gao, H. and Li, S., "A Wideband Printed Quadrifilar Helix Antenna under Frequency-Independent Dual Resonances". *Plasmonics*, 2018, *13*(6), pp.2141-2150.
17. Rabemanantsoa, J. and Sharaiha, A., "Size reduced multi-band printed quadrifilar helical antenna." *IEEE Transactions on Antennas and Propagation*, 2011, *59*, (9), pp.3138-3143.
18. Takacs, A., Fonseca, N.J. and Aubert, H., "Height reduction of the axial-mode open-ended quadrifilar helical antenna". *IEEE Antennas and Wireless Propagation Letters*, 2010, *9*, pp.942-945.
19. Hebib, S., Fonseca, N.J. and Aubert, H., "Compact printed quadrifilar helical antenna with iso-flux-shaped pattern and high cross-polarization discrimination." *IEEE Antennas and Wireless Propagation Letters*, 2011, *10*, pp.635-638.
20. Han, Y., Haoliang, W., Ziwei, W., Yuchen, Y., Yingjie, F., Kunkun, H., Yuan, G., Zhipeng, F. and Yuan, S., "Dual-band Spiral Printed Quadrifilar Helical Antenna Miniaturized by Surface and Inner Dielectric Loading." *IEEE Access*. 2019
21. Fartookzadeh, M., Mohseni Armaki, S.H.: "Wide-beam spiral antenna with three folded arms fed by compact three-way wilkinson power divider", *Electron. Lett.*, 2016, **52**, (8), pp. 587–588

Preprints (www.preprints.org) | NOT PEER-REVIEWED | Posted: 14 June 2019 doi:10.20944/preprints201906.0136.v1

22. Fartookzadeh, M., Mohseni Armaki, S. H.: "Wide-beam spiral antennas with multi-folded arms and compact feed networks for satellite application". 24th Iranian Conf. on Electrical Engineering (ICEE), IEEE Conf., Tehran, 2016, pp. 1661–1666